was chosen to show that the filter is capable of very good performance in terms of sidelobes. The expanded vertical scale of Fig. 17 proves the sidelobe levels to be lower than −30 dB. They actually may be lower than −40 dB because the two apparent sidelobes following the main compressed pulse at 25 ns intervals are not sidelobes but are internal reflections in the TWT amplifier used ahead of the oscilloscope as an aid to presentation.

Conclusion

The FTML technique appears well suited to a variety of problems requiring the generation of arbitrary, but continuous, delay characteristics over bandwidths of up to one octave. High losses and severe requirements on dimensional tolerances tend to limit the upper frequency range of usefulness of the technique to approximately 4 GHz. The lower-frequency limit is set by size and should be on the order of 100 MHz.

References

[1] V. E. Dunn, "A pulse compression filter employing a microwave helix," Stanford Electronics Labs., Stanford, Calif., Tech. Rept. 557-1, October 1960.

[2] H. S. Hewitt, W. R. Kincheloe, Jr., and M. H. Musser, "A study of several microwave compression filter techniques," Rome Air Development Center, Griffiss AFB, N. Y., Tech. Doc. Rept. RADC-TDR-64-398, November 1964.

[3] F. Mueller and R. Goodwin, "A wideband microwave compressive receiver," presented at IRE Internat'l Conv., New York, N. Y., March 26–29, 1962.

[4] H. S. Hewitt, "A design procedure for tapped-delay-line compression filters," Stanford Electronics Labs., Stanford, Calif., SEL-65-043 (TR1965-1), September 1965.

[5] "*Investigation of radar resolution and discrimination techniques*," Hazeltine Corp., Little Neck, N. Y., HRD Rept. 7816, December 1965 (Classified).

[6] J. H. Collins and G. G. Neilson, "Microwave pulse compression utilizing a yttrium iron garnet delay line," *Electronics Lett.*, vol. 1, p. 234, October 1965.

[7] V. E. Dunn, "Realization of microwave pulse compression filters by means of folded-tape meander lines," Stanford Electronics Labs., Stanford, Calif., SEL-62-113 (TR 557-3), October 1962.

Electromagnetic Resonances of Free Dielectric Spheres

MONIQUE GASTINE, LOUIS COURTOIS, AND JEAN LOUIS DORMANN

Abstract—**A systematic study is made of electromagnetic resonances of a spherical, free, and isotropic sample supposed to be without dielectric loss. The characteristic equation which is both complex and transcendant has been resolved with a computer. The results for the first modes (frequency and Q factor for ϵ varying between 1 and 100) are presented. The Q factor that is calculated represents the comparison between the energy stored by the resonance system and energy radiated per cycle; this is the theoretical maximum Q in the case of nonlossy materials.**

The different modes are classed in TE_{nmr} and TM_{nmr} modes which comprise exterior and interior modes. It is shown that for $n \geq r$ the energy is concentrated in all directions near the surface; these are known as surface modes. This systematic study is confirmed by experiments in which numerous modes have been observed and identified.

Introduction

THE LAST FEW years have seen the publication of several studies of electromagnetic resonances of free dielectric samples. This is explained by the high Q factor that can be obtained with a small space factor, when using high-dielectric constant materials and a low dissipation factor tan δ. The resonators used lend themselves to a number of different applications. However, their use requires a good knowledge of their spectra and field configurations.

A systematic study has been made of the resonances of an isotropic spherical dielectric sample, supposed without loss, placed in an infinite medium. This problem had only, until now, been studied by approximating a high ϵ relative dielectric constant.[1]–[6]

Manuscript received May 18, 1967; revised July 31, 1967.

The authors are with the Laboratoire de Magnetisme et de Physique du Solide, Centre National de la Recherche Scientifique, Bellevue, France.

Characteristic Equation

The dielectric sample creates in its proximity a concentration of semistationary electromagnetic energy. By using the Bromwich method, Maxwell's equations have been resolved taking into account the boundary conditions, zero energy at infinity. By using the spherical coordinates (ρ, θ, ϕ) it has been possible to class the waves as transverse electric modes (TE) and transverse magnetic modes (TM).

For a TE mode on the inside of the sample, the fields are

$$E_\rho = 0$$

$$E_\theta = -j\frac{km}{\rho \sin\theta}\sqrt{\frac{\mu}{\epsilon}}\sqrt{k\rho}\, J_{n+1/2}(k\rho) P_n^m(\cos\theta) \begin{matrix}\cos\\ -\sin\end{matrix} m\phi e^{j\omega t}$$

$$E_\phi = j\frac{k}{\rho}\sqrt{\frac{\mu}{\epsilon}}\sqrt{k\rho}\, J_{n+1/2}(k\rho) \frac{dP_n^m(\cos\theta)}{d\theta} \begin{matrix}\sin\\ \cos\end{matrix} m\phi e^{j\omega t}$$

$$H_\rho = \frac{n(n+1)}{\rho^2}\sqrt{k\rho}\, J_{n+1/2}(k\rho) P_n^m(\cos\theta) \begin{matrix}\sin\\ \cos\end{matrix} m\phi e^{j\omega t}$$

$$H_\theta = \frac{1}{\rho}\frac{d[\sqrt{k\rho}\, J_{n+1/2}(k\rho)]}{d\rho} \frac{dP_n^m(\cos\theta)}{d\theta} \begin{matrix}\sin\\ \cos\end{matrix} m\phi e^{j\omega t}$$

$$H_\phi = \frac{m}{\rho \sin\theta}\frac{d[\sqrt{k\rho}\, J_{n+1/2}(k\rho)]}{d\rho} P_n^m(\cos\theta) \begin{matrix}\cos\\ -\sin\end{matrix} m\phi e^{j\omega t}$$

where $P_n^m(\cos\theta)$ is the first kind associated Legendre function of orders n, m in $\cos\theta$, and $J_{n+1/2}(k\rho)$ is the first kind Bessel function of the order $n+1/2$ in $k\rho$ with $k=\omega(\sqrt{\epsilon\mu}/c)$ as the wavenumber in the dielectric sample.

Outside the sample, the expressions are similar in replacing the Bessel functions of the first kind by the Hankel functions of the second kind.

For the TM modes the expressions for the fields are the same when permutating the E and H fields and when taking into consideration the impedance $\sqrt{\mu/\epsilon}$.

The continuity conditions on the separation surface lead to a characteristic equation which is both complex and transcendental:

Mode TE_{nmr}

$$\frac{J_{n-1/2}(k\rho)}{J_{n+1/2}(k\rho)} = \frac{H^{(2)}_{n-1/2}\left(\frac{k\rho}{\sqrt{\epsilon}}\right)}{\sqrt{\epsilon}H^{(2)}_{n+1/2}\left(\frac{k\rho}{\sqrt{\epsilon}}\right)}$$

Mode TM_{nmr}

$$\frac{n}{k\rho} - \frac{J_{n-1/2}(k\rho)}{J_{n+1/2}(k\rho)} = \frac{n\epsilon}{k\rho} - \sqrt{\epsilon}\frac{H^{(2)}_{n-1/2}\left(\frac{k\rho}{\sqrt{\epsilon}}\right)}{H^{(2)}_{n+1/2}\left(\frac{k\rho}{\sqrt{\epsilon}}\right)}.$$

The resolution in

$$kR = X - jY = \frac{\sqrt{\epsilon\mu}}{c}R(\omega' - j\omega'')$$

where R, the radius of the spherical sample, and ω, the complex radian frequency, gives the free oscillation frequencies of the system and their relaxation times.

To help solve the equation we used a computer with a checkering method followed by a method of double iteration.

For each integer value $n \geq 1$ there is a corresponding discrete set of ω roots; the system is degenerate in m.

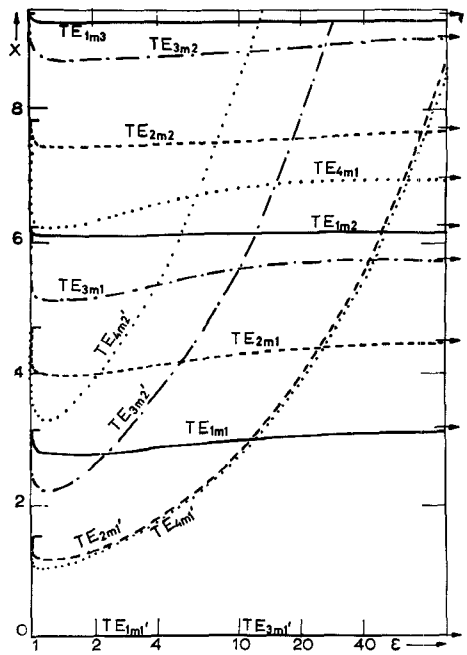

Fig. 1. The real part of characteristic equation solutions for TE modes with $n \leq 4$. $\omega = cX/R\sqrt{\epsilon\mu}$. The primed rs are for exterior modes.

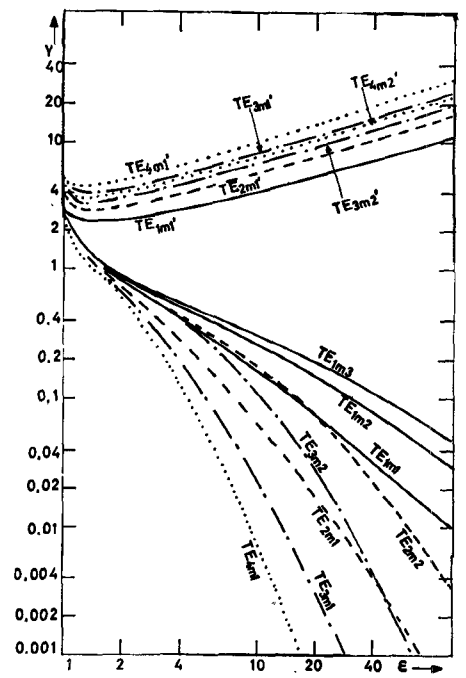

Fig. 2. The imaginary part of characteristic equation solutions for TE modes with $n \leq 4$. $Q = X/2Y$.

Figs. 1 and 2 represent the values of X and Y obtained for the TE modes of the order of $n \leq 4$. Figs. 3 through 10 represent those obtained for the TM modes.

For $\epsilon \to 1$, a direct derivation gives the solution $X = K\pi$ or $X = (2K+1)\pi/2$ where K is an integer.

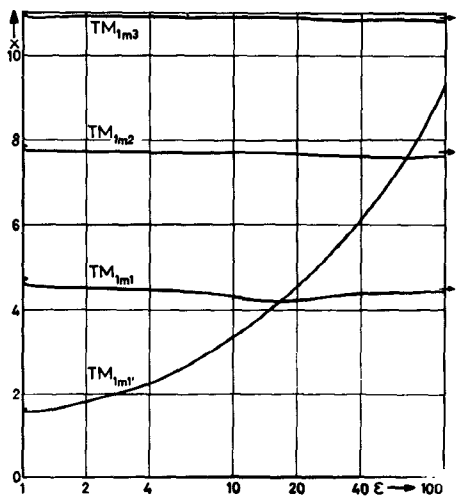

Fig. 3.

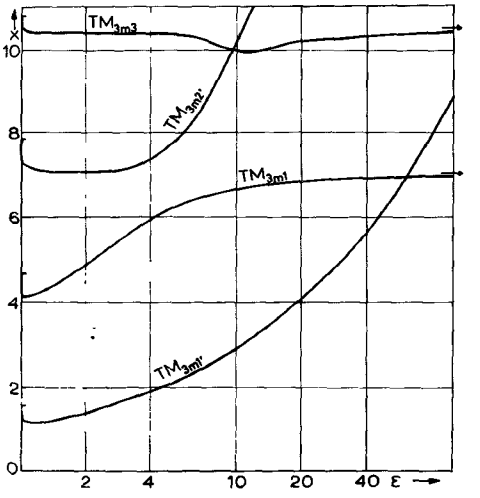

Fig. 5.

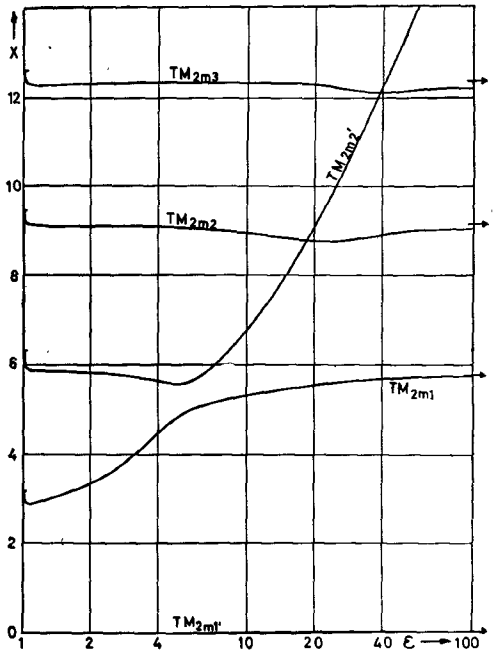

Fig. 4.

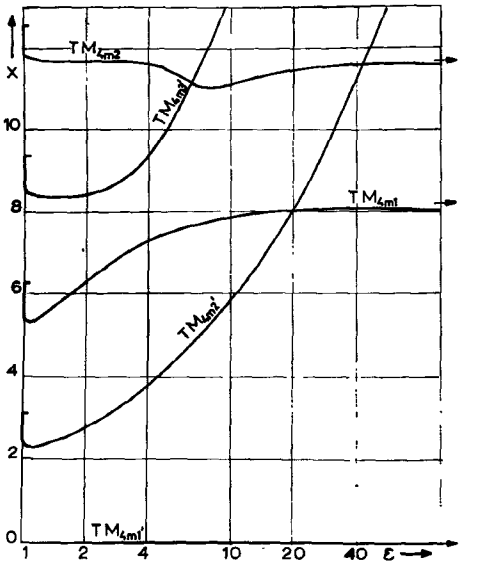

Fig. 6.

For $\epsilon \rightarrow \infty$, the solutions are either the zeros of the first kind Bessel function where the product kR is finite and real, or the zeros of the second kind Hankel function where the product $kR/\sqrt{\epsilon}$ is finite and complex.

This distinction is fundamental. The modes will be called "interior" when the product kR remains finite for $\epsilon \rightarrow \infty$, and "exterior" when the product kR tends towards infinity with ϵ. The order of the roots obtained has been labeled, respectively, the interior and exterior modes r and r'. In the two diagrams of the TE modes, the distinction between the two types is very clear whatever ϵ may be. It is not the same, however, on the diagram of the TM modes when coupling phenomenon appear between the two types; these then are mixed modes. The number of modes of the exterior type is limited, their number being given by the rule

Mode $TM_{nmr'}$

n odd: solution $X=0$ and $(n-1)/2$ other solutions

n even: $n/2$ solutions

Mode $TE_{nmr'}$

n even: solution $X=0$ and $n/2$ other solutions

n odd: $(n+1)/2$ solutions.

These two mode types can be explained physically by considering that on a diopter the incident rays are either in the least refractive medium or they are in the greatest refractive medium. In the same way, the interior modes shall be considered as a concentration of energy on the whole volume of the sample or on its surface but with a predominance of stored energy in the sample. However, it has been noticed

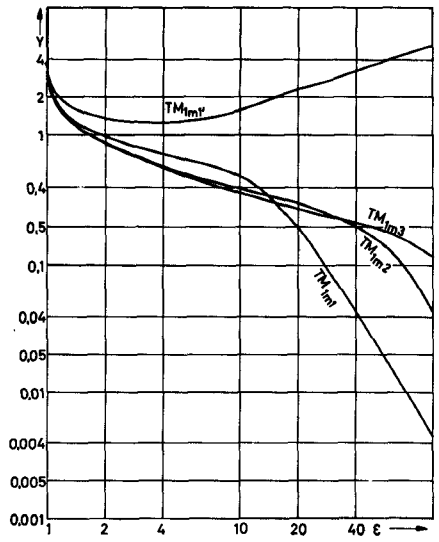

Fig. 7.

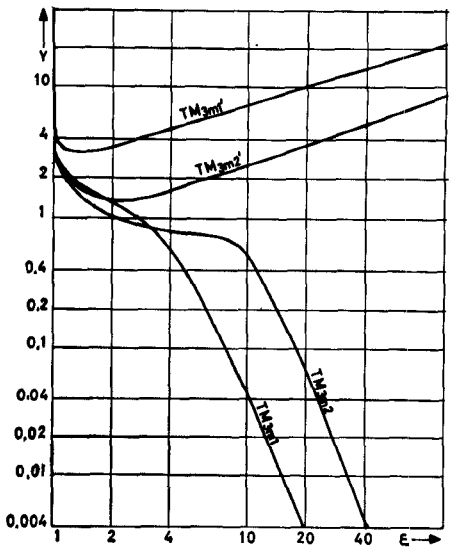

Fig. 9.

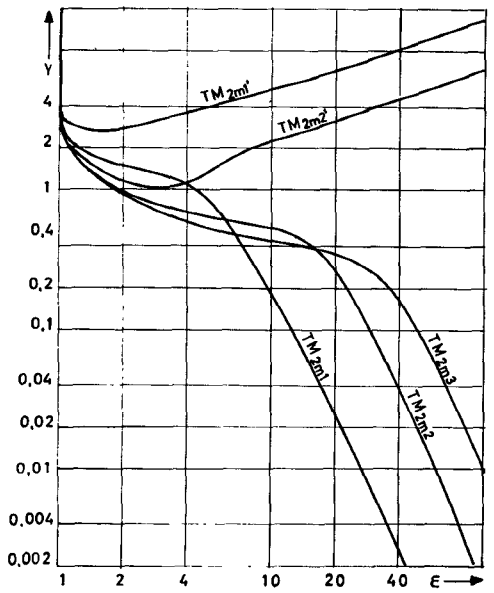

Fig. 8.

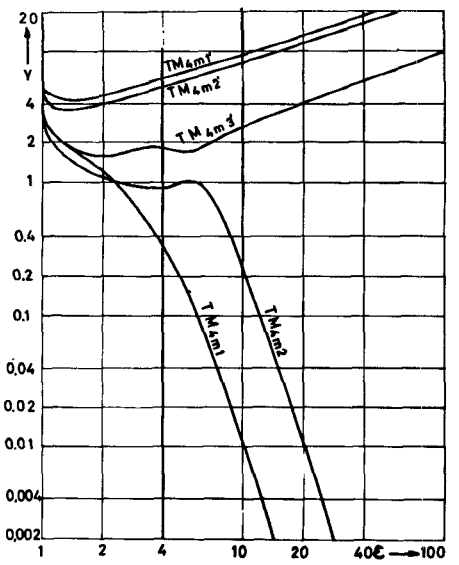

Fig. 10.

Figs. 3–10. The first TM solutions. Interior modes r and exterior modes r' present coupling phenomena.

that for the exterior modes the energy is only concentrated on the separation surface and more particularly outside the sample.

This becomes rigorous when $\epsilon \rightarrow \infty$. The refracting surface is then totally reflective and there may be waves on the outside (zero of Hankel function) and waves on the inside (zero of Bessel function).

Although the material losses($\tan \delta \rightarrow 0$) have been neglected, characteristic frequencies are found which are complex

$$\omega = \omega' - j\omega''.$$

This shows that there are "leaky modes." A Q factor can therefore be defined as

$$Q = \frac{\omega'}{2\omega''} = \frac{X}{2Y} = 2\pi \frac{\text{stored energy}}{\text{radiated energy per cycle}}.$$

The values of $X/2Y$ show that the Q of the exterior modes is always less than 1, whereas for ϵ greater than 5, the Q of the interior modes is greater than 10 and can even reach very high values. They are ∞ with $\epsilon \rightarrow \infty$.

This Q is the maximum theoretical Q obtained in the case of nonlossy materials. This value is of great interest since it indicates the possibility of coupling the mode to the exterior medium. A theoretical value for Q which is too low indicates a stored energy which is likewise too low, thus preventing the mode from being observed; hence, the exterior modes will never be observed.

A value for Q which is too large, however, ($Q > 1/\tan \delta$) indicates that the dielectric losses can no longer be neglected since they are more important than the radiation; such a mode also cannot be observed.

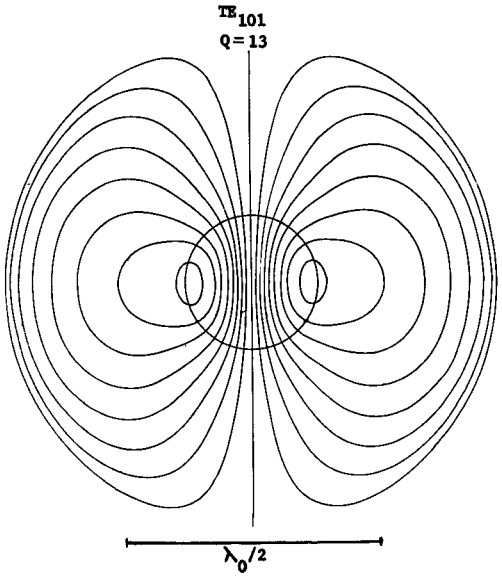

Fig. 11.

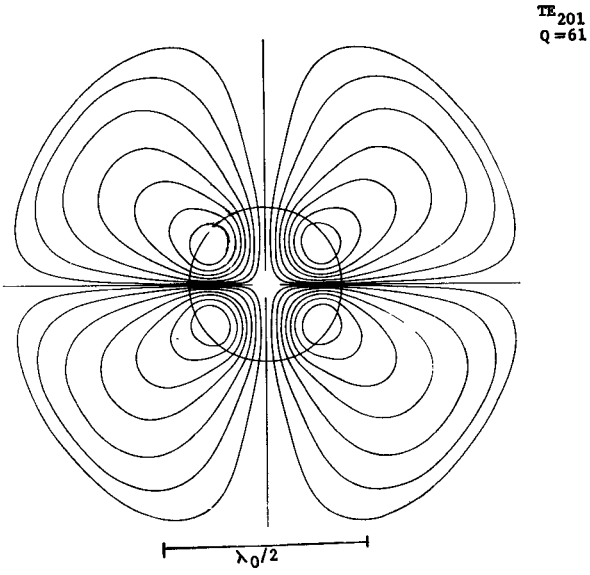

Fig. 13.

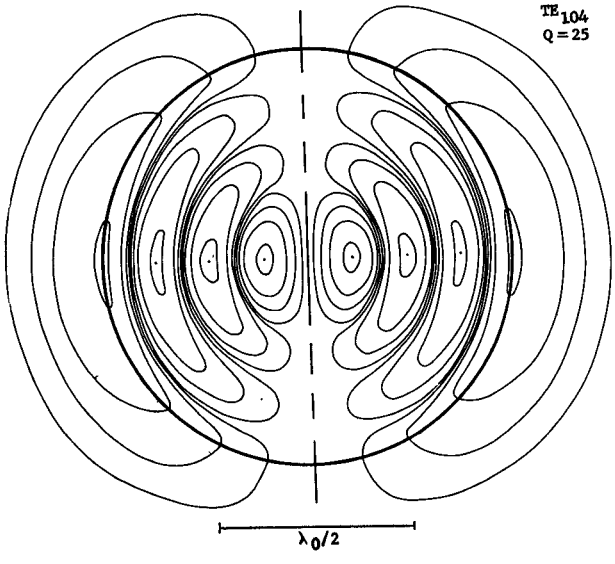

Fig. 12.

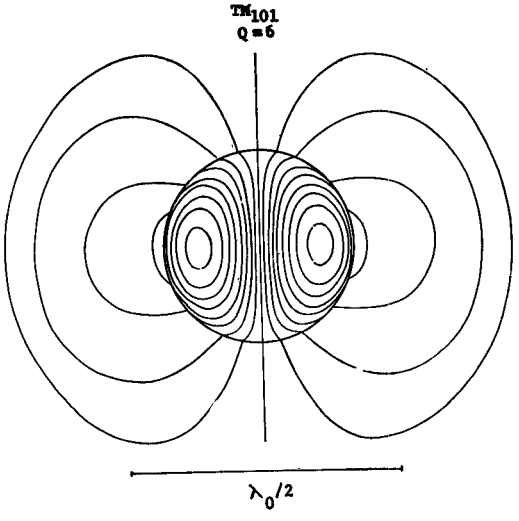

Fig. 14.

Figs. 11–14. Magnetic lines of force of the TE_{101}, TE_{104}, and TE_{201} modes, and electric lines of force of the TM_{101} mode.

Field Configuration

In an approximation of negligible radiation in comparison with the stored energy, we have studied the field configuration of the first interior modes on the interior of the dielectric as well as on the exterior.

For the TE modes the force lines of the electric field are on a sphere. In the case where m is zero the modes have a symmetry of revolution about the $\theta=0$ axis. The force lines of the electric field in this case are circles. The force lines of the magnetic field are situated in meridian planes.

Figs. 11 through 13 represent, as examples, the force lines of the magnetic field in a meridian plane for the TE_{101}, TE_{104}, and TE_{201} modes (using a dielectric sphere of constant $\epsilon=14$).

The drawing of the lobes outside the sample has been limited to those contained within the first spherical surface which behaves as a virtual "electric wall."

In the TM modes the nature of the force lines remains the same but the role of the H and E fields is permutated. Fig. 14 represents the force lines of the electric field of the TM_{101} mode.

In Figs. 15 and 16 the linear density of energy $H_\phi^2\rho^2$ and $E_\phi^2\rho^2$ has been represented as a function of the radial abscissa ρ. Here it is noticed that the modes can be classed as volume or surface modes according to whether $r \gg n$ or $n \gg r$; in the latter case the energy is concentrated in the proximity of the separation surface. The exterior modes are the first roots of the characteristic equation and it can be shown that they are always surface modes.

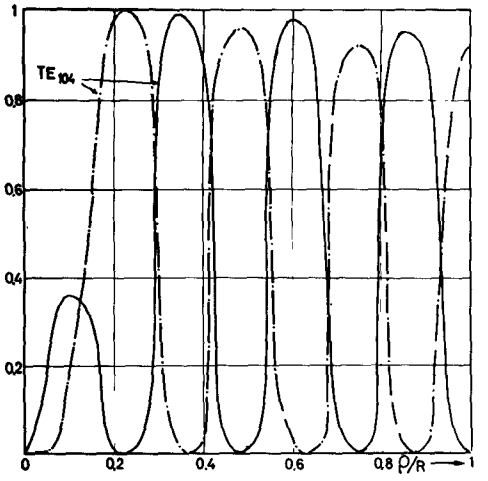

Fig. 15. Volume mode $n<r$.

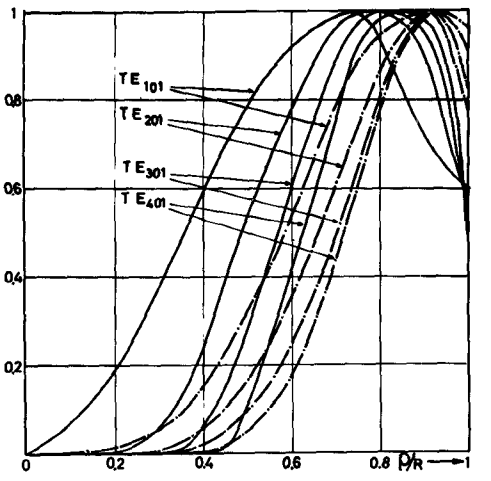

Fig. 16. Surface modes $n \geq r$.

Figs. 15–16. Magnetic energy density $H_\theta^2 \rho^2$ (solid lines) and electric energy density $E_\phi^2 \rho^2$ (dashed lines) in a direction θ versus normalized radial abscissa.

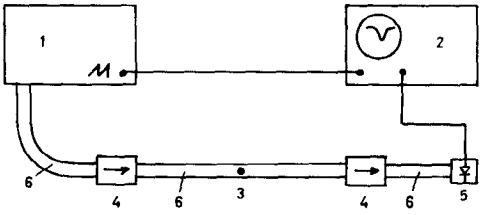

Fig. 17. Experimental setup in order to observe the dimensional resonances: 1) sweep generator; 2) oscilloscope or recorder; 3) sample under test; 4) isolator; 5) crystal detector; and 6) waveguide.

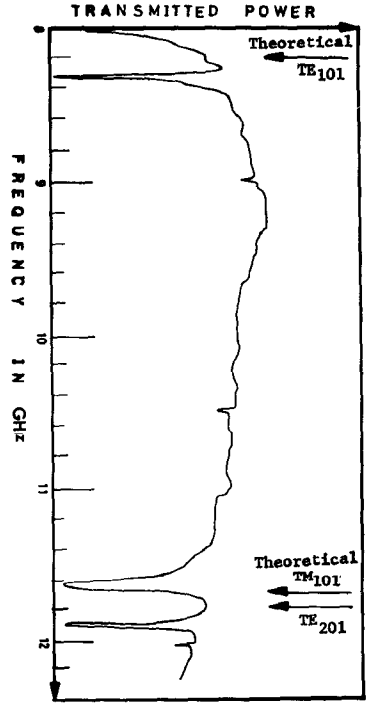

Fig. 18. Recording at the X band of the dimensional resonances of a dielectric sphere 3.9 mm in diameter, $\epsilon = 86$.

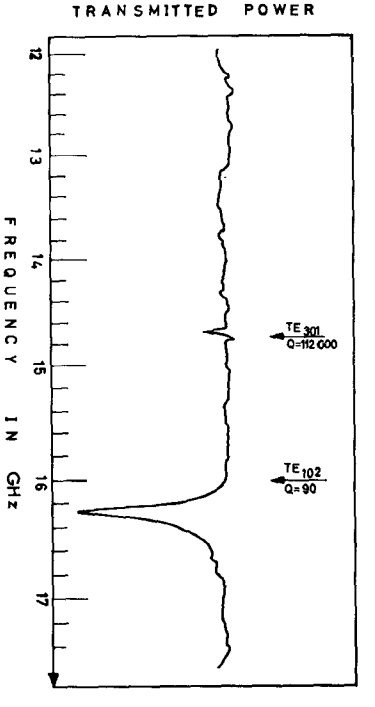

Fig. 19. Recording at Ku band of the dimensional resonances of a dielectric sphere 4 mm in diameter, $\epsilon = 86$.

Experimental Checking

These modes have been experimentally studied using a setup as shown in Fig. 17 at X and Ku bands.

Placing the sample in a waveguide removes the spherical degeneracy, the result being that each mode appears under the form of a set of three lines. However, for a good symmetrical position of the sample in the waveguide two of the three modes can be totally decoupled. For the $n=1$ modes, however, only a single line can never be decoupled.

Figs. 18 and 19 show the results obtained with a sphere 3.9 mm in diameter where $\epsilon=86$ at X and Ku bands. Verification is therefore excellent. These modes lend themselves to interesting applications such as measurement of small dielectric losses in material with a large dielectric constant.[7] The strong concentration of energy given by these modes has allowed us to build a power limiter using the TE_{101} mode of a YIG sphere.[8]

References

[1] P. Debye, "Der Lichtdruck auf Kugeln von behebigem Material," (in German *Ann. Phys.*, vol. 30, ser. 4, pp. 57–136, 1909.
[2] R. D. Richtmyer, "Dielectric resonators," *J. Appl. Phys.*, vol. 10, no. 6, p. 391, June 1939.
[3] J. A. Stratton, *Electromagnetic Theory*. New York: McGraw-Hill, 1941, p. 554.
[4] A. Okaya, "The rutile microwave resonators," *Proc. IRE* (*Correspondence*), vol. 48, p. 1921, November 1960.
[5] A. Okaya and L. F. Barash, "The dielectric microwave resonator," *Proc. IRE*, vol. 50, pp. 2081–2092, October 1962.
[6] H. Y. Yee, "An investigation of microwave dielectric resonators," Microwave Labs., Stanford University, Stanford, Calif., Rept. 1-065, July 1963.
[7] R. O. Bell and G. Rupprecht, "Measurement of small dielectric losses in material with a large dielectric constant at microwave frequencies," *IRE Trans. Microwave Theory and Techniques*, vol. MTT-9, pp. 239–242, May 1961.
[8] L. Courtois, "A new low level limiter for centimeter and millimeter waves," *J. Appl. Phys.*, vol. 38, pp. 1415–1476, March 1967. Also presented at 12th Annual Conf. on Magnetism and Magnetic Materials, Washington, D.C., November 15–18, 1966.

A High-Power UHF Circulator

YOSHIHIRO KONISHI, SENIOR MEMBER, IEEE

Abstract—**The insertion loss, the bandwidth ratio, and the nonlinearity of a high-power UHF circulator are discussed generally with regard to the characteristics, volume, and filling factor of the ferrite. Theory and experiment are made on the high-power circulator with ferrite, where either surface of the ferrite comes into contact with air. A wideband technique in improving the narrowband that is essentially the result of the filling factor of ferrite is also described.**

To avoid the center conductor heating effect, a circulator without a center conductor is described.

Experiments have proven that, for ferrite nonlinearity, the threshold power by spinwave occurs in a polycrystal for CW power even above resonance and is changed by a external field strength, whereas the nonlinearity is not observed in a single crystal.

I. Introduction

THE ORDINARY Y-stripline circulator has been developed and studied by many authors.[1]–[5] However, in the case of a high-power CW circulator important factors for practical use such as temperature rise, ferrite nonlinearity, bandwidth, and insertion loss have not been adequately explained. As an example, nonlinearity occurs in a polycrystal at a comparatively low-power CW even under an above resonance operation, although such a phenomenon is not observed in a single crystal.

First, the general relation between several electrical characteristics of a circulator is studied in Section II. As a result, it becomes clear that the ferrite of the volume necessary for linearity should come into contact with as wide a surface as possible for good heat conductivity. It is also clarified that insertion loss depends only on ηQ values of the ferrite material reaching a minimum value at the optimum external field, and further, that the bandwidth ratio is related to the filling factor of the ferrite.

Second, to satisfy the general requirements already mentioned, analysis is made for the circulator in which either surface of a ferrite plate comes into contact with a small dielectric constant and permeability, such as air, to create a wide surface and volume of ferrite. Wideband techniques to improve the narrowband, essentially caused by the filling factor of the ferrite, are described. For practical use, construction that offsets rising temperature as a result of the center conductor is also considered.

Finally, several experiments confirming both theory and practical use are described.

Manuscript received May 17, 1967; revised August 7, 1967.
The author is with the Technical Research Laboratories, Nippon Hoso Kyokai, Tokyo, Japan.

II. General Considerations

The approximate values of the characteristics of a circulator such as insertion loss L (decibels), bandwidth ratio w, and available maximum power P_{crit}, are obtained by relating the volume τ and the filling factor k_f (=the time average magnetic energy $\bar{W}_m$/time average total magnetic energy $\bar{W}_{mt}$) of the ferrite contained in a symmetrical 3 port under the following assumptions:

First, it is assumed that there exists no magnetic energy inside the ferrite under the same-phase excitation. This assumption is satisfied for the lumped element Y circulator[7]